China Ocean Eng., Vol. 30, No. 6, pp. 916 – 925

DOI 10.1007/s13344-016-0059-x, ISSN 0890-5487

Design of Measuring Instrument with Whole Direct Method for Bed Shear Stress Under Two-Dimensional Water–Flow Co-action*

HUANG Hai-long (黄海龙)[a, b, 1], ZUO Qi-hua (左其华)[a, b], ZHOU Yi-ren (周益人)[a, b], SHEN Yu-sheng (沈雨生)[a, b] and LI Lan-xi (李蓝汐)[c]

[a] *Nanjing Hydraulic Research Institute*, *Nanjing 210029*, *China*

[b] *Key Laboratory of Port*, *Waterway and Sedimentation Engineering of MOT*, *Nanjing 210024*, *China*

[c] *Business School*, *Hohai University*, *Nanjing 210098*, *China*

(Received 20 October 2015; received revised form 22 February 2016; accepted 20 March 2016)

ABSTRACT

The present study aims at the design and making of measuring instrument of whole direct method for bed shear stress under two-dimensional water–flow co-action. The instrument combines the traditional strain gauge with a precise pressure gauge, and adopts the method directly measuring the difference between the lateral hydrodynamic pressure and different head pressures on both sides of the force plate. As a result, such an instrument solves a technical puzzle of the past strain gauge, i.e. the difficulty to set apart shear stress and lateral force. Static force test and sink test both prove that the instrument is precise, stable and applicable to the measurement of rough beds with different shear stresses.

Key words: *direct method*; *shear stress*; *measurement*

1. Introduction

River and costal evolution is directly related to sediment movement, bottom sediment movement in particular. However, sediment movement is constrained by the magnitude of bed shear stress under water–flow action. In this case, research on bed shear stress is one of the important approaches to study the fundamental theoretical issues concerning sediment movement.

There are two major categories of measurement of bed shear stress: one is indirect measurement, and the other is direct measurement.

The indirect measurement method firstly tests the physical quantity of water–flow movement property, and further deduces bed shear stress based on relevant theories. The fundamental theoretical basis is $\tau = \upsilon \partial U / \partial Z$, in which υ is the coefficient of viscosity of medium. In aerodynamics, wind shear stress is usually determined with such a method. The earlier qualitative measurement also employs methods of similar type, for example, the method of producing bubbles from bed, and that of small ball placement. Sleath (1988) derived bed shear stress under turbulent flow action from measuring the fluctuating velocity on the horizontal direction inside the boundary layer. Recently, with

* This work was financially supported by the National Major Special Project for Scientific Instruments and Equipment Development "Intelligent Measurement and Control System Development for Large-Scale River Model Tests in China" (Grant No. 2011YQ070055).

1 Corresponding author. E-mail: hlhuang@nhri.cn

the aid of thermal aerodynamic measurement of shear stress in the field of aviation, Liang *et al.* (2010) have conducted measuring experiment study of shear stress under water–flow co-action. The indirect measurement method can adopt relatively reliable measures to acquire the physical quantity of medium movement property with high precision. Nevertheless, some fundamental theoretical bases have come from the unverified assumptions; therefore, some kinds of empirical coefficients might be introduced so as to influence the validity of test results.

The direct measurement method is used to determine bed shear stress with different roughnesses. Early in 1966, Jonsson (1966) measured the hydrodynamic property of wave boundary layer with direct measurement method and estimated the bottom friction coefficient. Riedel *et al.* (1972) and Kamphiuls (1975) measured bed shear stress and bottom friction coefficient under oscillatory wave action with direct measurement method. Rankin *et al.* (1998) measured bed shear stress under moving bed condition; Mirfenderesk (2003) also directly measured shear stress of both smooth bed and rough bed with shear stress plate. Since 1990, quite some researches have been done to measure bed shear stress in China. Based on the past research on measuring shear stress, Qin and Zhao (1993) analyzed the potential measurement errors and developed the shear stress gauge of strain type, and improved the gauge in 1999 (Qin *et al*., 1999). In the past few years, Cai (2007) has designed and made a set of devices to measure shear stresses. Such devices can also be used to measure bed shear stress under wave action at different time.

The direct measurement of bed shear stress under wave action is mainly applied to solving the difficult issue of dynamic water separation along the fluid motion direction acting on the side wall of the experiment plate and on the strain gauge. Riedel *et al.* (1972) employed the way of increasing the length of experimental bed so that the hydrodynamic force on the side wall is small enough compared with the bed shear stress; therefore, major errors could be circumvented. In the same vein, Qin and Zhao (1993) obtained the horizontal action force and decreased its influence with theoretical calculation. In fact, the actual action is not known. The measurement is still indirect. Most of the other studies did not take this factor into consideration. Another factor affecting the measurement of bed shear stress is the interference for shear stress on the vertical direction. Qin and Zhao (1993) employed the method of placing the experimental bed on a ball, but in this way, when acting on waves, due to the differences of water head and the existence of the vertical hydrodynamic force in front of and behind the force plate, the result is definitely less desirable compared with that under the one-directional fluid action condition. It is difficult to solve the two key problems concerning the research on shear stress instrument.

As the research to date has inadequacies, this paper aims to analyze the influence of different factors on bed shear stress measurement. Direct measurement method was employed to obtain each quantity affecting bottom shear stress instrument, and eventually net bottom shear stress was separated so as to be applied to lab research for hydrodynamics.

2. Methods

2.1 Acting Force Analysis of Measuring Instrument

Fig. 1 shows the horizontal acting force on a measuring instrument. The lateral shear stress acting

on the side walls of the panel, parallel to the water–flow action direction, can be neglected as the lateral shear stress along the water–flow action is relatively small, because the walls are smooth and the stress surface is smaller than the plate surface (usually 1% of the plate surface area).

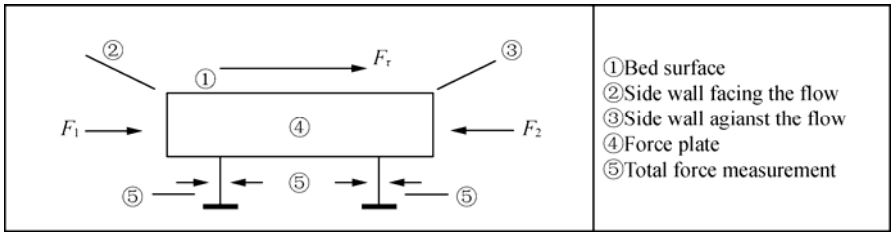

Fig. 1. A diagram of horizontal acting force on the force plate.

If the bed surface force plated is used to connect the upper and bottom parts, the influence of static water pressure on both sides of the measuring instrument can be neglected. Only the hydrodynamic pressure influence along the uneven vertical direction of the bed surface should be taken into consideration.

The horizontal forces acting on the measuring instrument include:

$$F = F_\tau + F_1 - F_2 + \Delta F \,, \tag{1}$$

where, F stands for the total force obtained by the force plate; F_τ is the needed shear stress; F_1 is the horizontal force from the flow coming direction; F_2 is the horizontal force against the flow coming direction (see Fig. 2); ΔF is the net horizontal force acting on the measuring instrument. F_1 and F_2 comprise the hydrodynamic force and static water pressure. Under the water–flow action, the static water pressures of F_1 and F_2 offset each other; however, if influenced by wave action, such two static water pressures cannot offset each other. When the bed surface reaches certain thickness, the vertical distribution of hydrodynamic pressure along the bottom bed template should be taken into consideration.

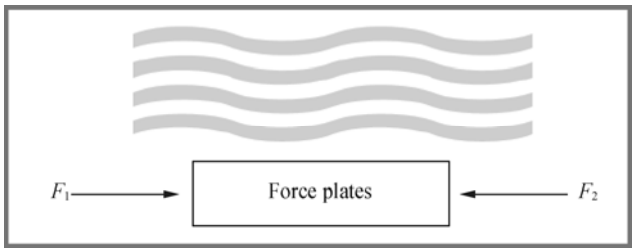

Fig. 2. A diagram of F_1 and F_2 action under wave action.

2.2 Measurement of F_1 and F_2

F_1 and F_2 are represented by the following formula:

$$F_i = (F_\mathrm{d})_i + (F_\mathrm{h})_i \qquad i = 1, 2 \tag{2}$$

where, F_d is the hydrodynamic pressure acting on the front and rear side walls of the force plate; F_h is the static water pressure acting on the front and rear side walls. i stands for both sides of the force plate,

i=1 is the flow coming direction; i=2 is the anti-water-coming direction.

Under the wave action, there is wavefront phase difference between the front and rear ends of the force plate, the hydrodynamic pressure and the static water pressure on the front and rear side walls are inconsistent. The magnitude of the phase difference is related to the ratio of the length of the force plate to the length of incident wave. In this case, when designing the measuring instrument, on the one hand, appropriate length of the plate should be considered to decrease the influence of phase differences, on the other hand, the acting force caused by water head pressure at both ends of the force plate should be measured directly. As water pressures on all directions are of the same nature, a pressure gauge should be placed at the bottom of the force plate to implement the measurement. And the following formula can be obtained:

$$F_{\mathrm{h}} = (F_{\mathrm{h}})_1 - (F_{\mathrm{h}})_2 . \tag{3}$$

Although the distance between the ends of the force plate and the model room is very small (calculated at the level of millimeter), there exists the influence of dynamic pressure, and the vertical distribution along the plate thickness varies. As the force plate usually simulates the typology of different roughnesses, the plate cannot be too thin. If the force plate is divided into two parts along the thickness direction, one part is thin enough so that the influence of the vertical distribution of hydrodynamic force can be neglected. As a result, the average pressure of several points $\overline{p}$ can be obtained and the water dynamic force on this part of the area Δs can be further acquired:

$$F_i = \overline{p}\Delta s . \tag{3}$$

On the other part, the separation wall would take and decrease dynamic pressure so that this part of the force plate will take the water head pressure, as shown in Fig. 3.

The stilling room plays the role in taking both the force plate action and the dynamic water action on the measuring instrument. It can also allow sediment to go through the crack between the force plate and the model room and enter the measuring room so as to influence the measuring force.

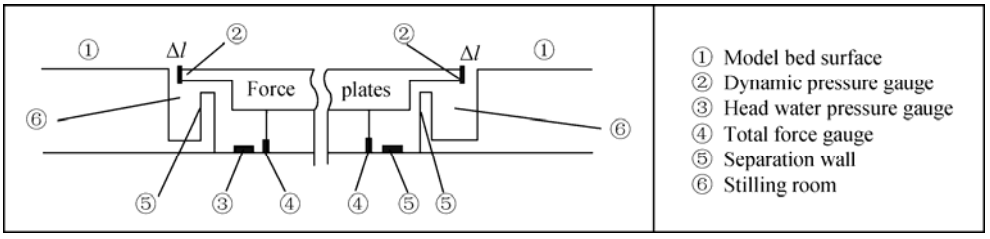

Fig. 3. A diagram of top division of the force plate and force measurement.

2.3 Determination of Net Water Pressure

If the measuring room is connected to the outside water, and the measuring instrument is very small, the ratio of hydrodynamic force to total force acting on the measuring instrument can be neglected; however, the head water pressure on both sides of the instrument can offset each other. That means:

$$\Delta F \approx 0 . \tag{5}$$

2.4 Determination of the Length of the Force Plate L_B

On the one hand, the force plate should be long enough to simulate the bed surface of different roughnesses. In other words, the longer the force plate is, the more precise the shear stress of the simulated bed surface. In this case, the ration of the lateral action force to the shear stress will decrease and subsequently, the measuring precision of the shear stress will be improved. Jonsson (1966) chose a 0.875 cm-long force plate. On the other hand, if the forces (vertical force included) taken by both ends of the force plate differ too much, the vertical force and the horizontal force may greatly interfere with each other. The length of the force plate is usually decided empirically in the range of 0.2–0.4 m.

According to Fig. 3, the ratio of L_B to the wave length L should avoid the value around 0.25 or that around 0.5. When a period is relatively long, L_B can be 1/8. When wave period is smaller than 1.0 s, it can be (0.75–1.0)L.

2.5 Interference with the Horizontal Force by the Vertical Force

First of all, the unevenness of the vertical forces acting on both ends of the force plate should be decreased, and the differences of the forces should be minimized. Also, the multi-point measurement should be adopted so as to keep the force plate stable. In the end, the multi-point measuring force plate should be connected in bridge-road manners in order to eliminate their mutual interference.

2.6 Determination of the Maximum Shear Stress $|(F_\tau)|_{max}$

The force obtained by the measuring instrument is the total shear stress acting on the force plate. When the maximum shear stress is needed in a test, the following formula can be employed:

$$F_\tau(t)=\int_0^{L_B}F_\tau(t,x)\mathrm{d}x\,. \tag{6}$$

Based on relevant theories, $F_\tau(t,x)$ satisfies the following formula:

$$F_\tau(t,x)=f_w U_b|U_b|. \tag{7}$$

Under certain wave and bed conditions, f_w can be considered a constant. From the distribution of U_b, the phase positions of the maximum and the minimum value of $F_\tau(t,x)$ can be derived, and the maximum shear stress and its acting point can be further obtained. A wave gauge can be placed on both ends of the force plate respectively, and therefore, the wave height corresponding to the shear stress can be accurately decided.

3. Development and Calibration of Model Instrument

3.1 Basic Structure

The properties of the test basin and wave generator are taken into consideration, and the size of measuring platform is 200 mm×400 mm×40 mm, placed inside a 220 mm×420 mm rectangular framework (see Figs. 4 and 5). The distance between the framework and the force plate is 1 mm.

The force plate is 10 mm thick and 15 mm long with the front of its ends divided into 2 mm-upper part and 8 mm-lower part. There are two through holes with the diameter of 2 mm on the upper part of

the force plate ends, with a high-precision pressure sensor in each through hole.

The total force measuring instrument consists of four high-precision strain sensors, and they, together with the force plate, constitute a force measuring platform. The electric circuit adopts bridge design. The whole bridge design or half bridge design as it may be, the output voltage and the resistance change of the high-precision pressure sensor all change in linear manners.

The measuring platform consists of four strain sensors with the total range being 2000 g and the resolution ration of 2 g.

The basic structure of the measuring instrument can be referred to Figs. 4 and 5.

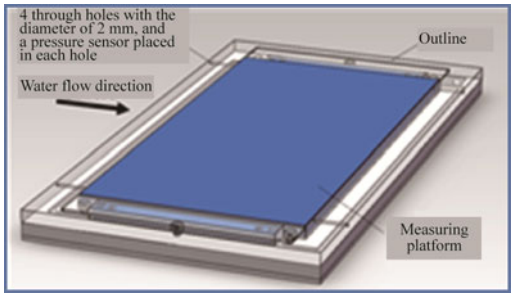

Fig. 4. The outside view of the measuring instrument platform.

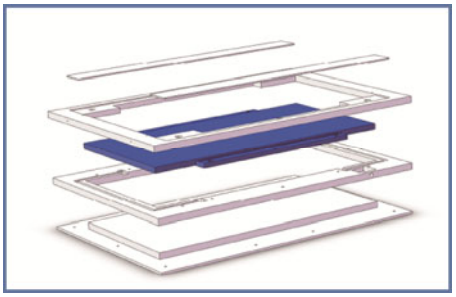

Fig. 5. The inner structure of the measuring instrument.

Table 1 lists the performance parameters of the measuring instrument.

Table 1 Performance parameters of the measuring instrument

Measuring area	200 mm×400 mm
Horizontal force range	2 kg
Comprehensive precision	＜0.2% F.S.
Sensitive quality	≤5 g
Overload capacity	150% F.S
Levels of protection	IP68 (within 5 m underwater)
Sampling frequency	10–5000 Hz multi-level choices
Resolution ration	16-bit AD
Bus interface	RJ45 (standard web interface)

3.2 The Calibration and Errors of the Measuring Platform

3.2.1 *Static Calibration*

Fig. 6 shows the general structure of static calibration system, including static calibration platform, measuring platform sensor, signal measuring and magnifying devices, A/D data collection card, and computer data collection and processing software.

Two weights, one of 500 g and the other of 1500 g, were added to the measuring platform, and the measurement was conducted twice. Table 2 presents the data obtained from the two measurements in which the weights were added to the measuring platform. The non-linear errors, repeatability errors and hysteresis errors of the above data were analyzed, and the sensor error data were obtained as shown in Table 3. The analysis shows that it is feasible to analyze errors of the calibrating measuring platform with weights. This test proves the adaptability of calibrated matrix in platform measurement.

The comprehensive precision of the measuring platform is smaller than 0.2%F.S which generally satisfies the test requirements.

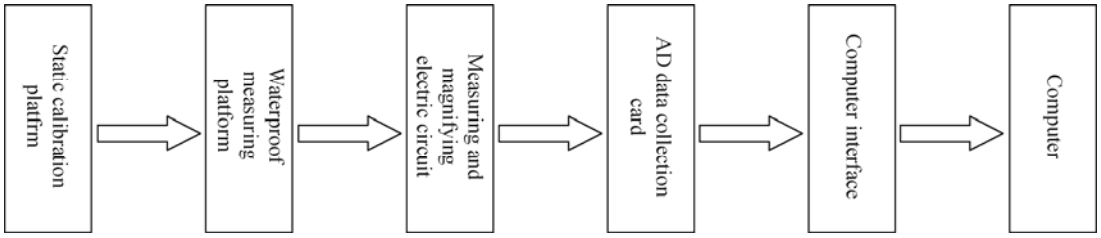

Fig. 6. A diagram of static calibration system components.

Table 2 Test data of the measuring platform with added weights

	Displayed force (g)	Actual added force (g)	Error (g)
First travel	498.0	500	2.04
	1002.1	1000	–2.08
	1501.0	1500	–1.02
	999.0	1000	1.02
	501.0	500	–1.02
Second travel	499.0	500	1.02
	1001.0	1000	–1.02
	1499.0	1500	1.02
	1002.0	1000	–2.04
	501.0	500	–1.02
Maximum value	1501.0	1500	2.08

Table 3 Error analysis

	Maximum value (g)	Designed range (g)	Precision (%)
Non-linearity	2.08	2000	0.10
Repeatability	3.06	2000	0.15
Hysteresis	3.10	2000	0.16

4. An Application Case

The actual measurement was conducted in a basin of Nanjing Hydraulic Research Institute. The needed wave-flow environment can be simultaneously generated for the current test. The front and rear bed surface in the test area is of cement plaster, and the side walls are made of glass frame structure. The wave height was measured by CBY-Ⅱ wave measurement control system developed by Nanjing Hydraulic Research Institute. The velocity was measured by ADV with the precision of ±1 mm/s.

In order to simulate the roughness of the bed surface, some crushed stones were attached to the surface of the measuring platform and the front and rear test area (see Fig. 7). With such a measuring platform, single water flow, single wave, and the bed shear stress under wave-flow co-action were tested respectively. The sampling frequency was set up at 100 Hz.

4.1 Water Flow Action

The test on single water flow action included two water depths, 0.15 m and 0.45 m, respectively.

The velocities under 0.15 m water depth included three types, 0.25 m/s, 0.51 m/s and 1.06 m/s; the velocities under the water depth of 0.45 m also included three values, 0.23 m/s, 0.43 m/s and 0.77 m/s.

The results of the measuring bed shear stress under single water–flow action can be found in Table 4. Fig. 8 presents the relationship between the velocity and the shear stress.

Fig. 7. Layout of the actual measurement.

Table 4 Test results of the bed shear stress under single water–flow action

Water depth h (m)	Velocity v (m/s)	Results of the bed shearing force measurement (g)	Results of the bed shear stress measurement (N)
0.15	0.25	11	1.35
	0.51	43	5.27
	1.06	195	23.89
0.45	0.23	6	0.74
	0.43	30	3.68
	0.77	90	11.03

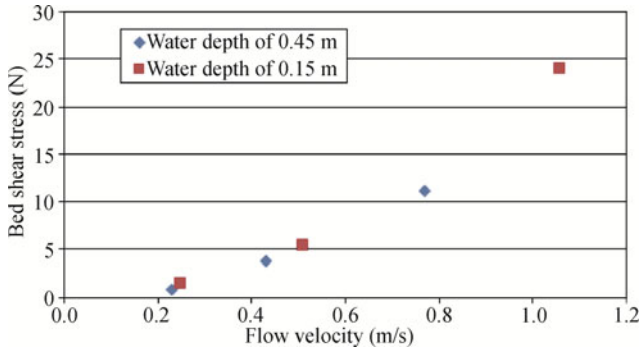

Fig. 8. Relationship between velocity and shear stress.

From the test results, the larger the velocity is, the larger the bed shear stress is. This conforms to the generally regular pattern.

4.2 Wave Action

The test results of the bed shear stress under single wave action can be found in Table 5. Fig. 9 presents the relationship between the wave height and the shear stress.

According to the test results, in the same wave period, the larger the wave height is, the larger the bed shear stress is; for the same wave height, when the wave period is relatively small (T=0.8 s), the bed shear stress is relatively small.

Table 5 Test results of the bed shear stress under single regular wave action

Water depth h (m)	Wave		Results of bed shearing force measurement (g)		Results of bed shear stress measurement (N)	
	Wave height H (cm)	Period T (s)	Positive	Negative	Positive	Negative
0.45	3.5	1.5	31	–25	3.80	–3.06
	5.5		53	–41	6.49	–5.02
	7.0		64	–47	7.84	–5.76
	5.5	0.8	17	–16	2.08	–1.96
		2.5	46	–28	5.64	–3.43

Note: The positive value of the shear stress means following the wave direction; the negative value indicates the anti-wave direction.

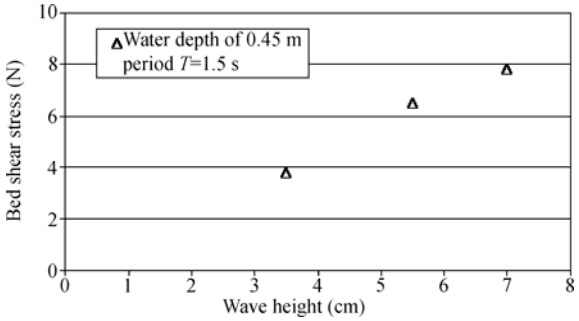

Fig. 9. Relationship between wave height and shear stress.

4.3 Water–Flow Co-action

The test of water–flow co-action was conducted under certain water flow, in which different wave elements were added together. The wave depth was 0.45 m, and the flow velocity was 0.43 m/s. Regular waves were employed with the wave period T=1.5 s and the wave heights of 2.7 cm, 4.0 cm, and 5.0 m, respectively.

The test results of bed shear stress under water–flow co-action can be found in Table 6.

Table 6 Test results of bed shear stress under water–flow co-action

Water depth h (m)	Flow velocity v (m/s)	Wave		Results of bed shearing force measurement (g)		Results of bed shear stress measurement (N)	
		Wave height H (cm)	Period T (s)	Peak value	Valley	Peak value	Valley
0.45	0.43	2.7	1.5	55	11	6.74	1.35
		4.0		69	–4	8.45	–0.49
		5.0		78	–7	9.56	–0.86

Based on the test results, in the same wave period, the larger the wave height is, the larger the bed shear stress is. Fig. 10 shows the hydrograph of the bed shearing force under water–flow co-action.

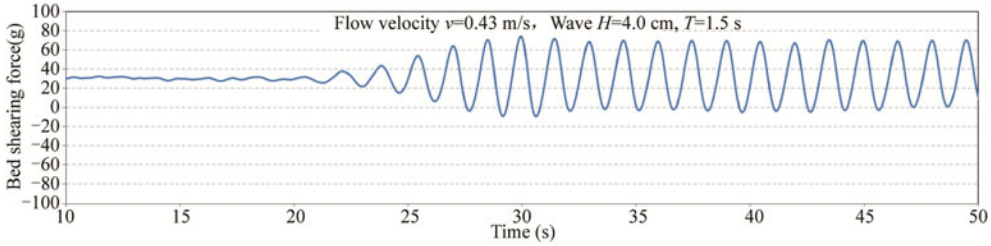

Fig. 10. Hydrograph of the bed shearing force under water–flow co-action.

5. Conclusions

(1) The shear stress measuring instrument of pressure type developed in the present study overcame the weaknesses of the past direct shear stress measuring instrument. It has relatively high static precision and can be applied to measuring shear stress of bed surfaces with different roughnesses.

(2) By a series of actual tests on wave action, flow action and wave-flow co-action, the test results of shear stress measuring instrument showed the desirable systematicness and relativity. Nevertheless, the tested value should be further compared with the calculated value and actually tested value with the aid of other instruments so that the precision and errors in dynamic measurement can be fairly analyzed and determined.

(3) In future tests, the pressure difference on device ends should be tested at the same time, analyzed together with the actual value synchronously in order to separate and assess the potential influence from the horizontal pushing force on the shear stress test value.

References

Cai, C. F., 2007. *Experimental Study of Bottom Friction Coefficient and Sediment Starting Force Under Wave Action*, MSc. Thesis, Hohai University, Nanjing. (in Chinese)

Jonsson, I. G., 1966. Wave boundary layers and friction factors, *Coastal Engineering Proceedings*, **1**(10): 127–148.

Kamphiuls, J. W., 1975. Friction factor under oscillatory waves, *J. Waterw. Port Coast. Ocean Eng. Div.*, ASCE, **101**(2): 135–145.

Liang, T., Xia, Y. F. and Xu, H., 2010. Preliminary study of bed shear stress measurement under wave action, *Journal of Waterway and Harbor*, **10**(5): 425–425. (in Chinese)

Mirfenderesk, H. and Young, I. R., 2003. Direct measurements of the bottom friction factor beneath surface gravity waves, *Appl. Ocean Res*., **25**(5): 269–287.

Qin, C. R., Qiu, X. Y., Li, D. J. and Zhao C. J., 1999. Study on bottom shear stress of laminar boundary layer under the action of random waves, *Journal of Hydraulic Engineering*, **30**(12): 48–51. (in Chinese)

Qin, C. R. and Zhao, C. J., 1993. Experimental investigation on the bottom shear stress of the sand ripple bed under wave action, *Journal of Hydraulic Engineering*, (9): 2–10. (in Chinese)

Rankin, K. L., Bruno, M. S. and Hires, R. I., 1998. Measurement of shear stress on a moveable bed, *Proceedings of the 24th Conference on Coastal Engineering*, ASCE, 2629–2639.

Riedel, P. H., Kamphuis, J. W. and Brebner, A., 1972. Measurement of bed shear stress under wave, *Proceedings of the 13th Conference on Coastal Engineering*, ASCE, 587–603.

Sleath, J. F. A., 1988. Transition in oscillatory flow over rough beds, *J. Waterw. Port Coast. Ocean Eng.*, ASCE, **114**(1): 18–33.